



In Vitro Biocompatibility and Antimicrobial activities of Zinc Oxide Nanoparticles (ZnO NPs) Prepared by Chemical and Green Synthetic Route— A Comparative Study

Mahalakshmi S¹ · Hema N¹ · Vijaya P.P¹

Published online: 23 November 2019

© Springer Science+Business Media, LLC, part of Springer Nature 2019

Abstract

Zinc oxide nanoparticles (ZnO NPs) have emerged as a good anticancer and antibacterial activity, which are involved with their strong ability to trigger excess reactive oxygen species (ROS) production, release zinc ions and induce cell apoptosis. The present study aims to synthesize ZnO nanoparticles from zinc acetate (chemical co-precipitation method), and green synthesis (Sesbania grandiflora leaf extract) method evaluated their antibacterial and hemolytic activities. The prepared ZnO NPs were characterized by various techniques such as UV-visible absorption spectroscopy, X-ray diffraction (XRD), field emission scanning electron microscope (FE-SEM), energy dispersive X-ray analysis (EDX), high-resolution transmission electron microscope (HR-TEM) and Fourier transform infrared spectroscopy (FTIR). FE-SEM study reveals that the morphology of the crystal is spherical and flakes-shaped and the estimated sizes were 70–150 nm. The analysis of EDAX has shown the presence of zinc and oxygen. The HR-TEM analysis of zinc oxide nanoparticles with different magnifications consists of spherical shape and it is well distributed without any aggregation. The FTIR study has shown the presence of Zn–O bond, C–O bond, C–H bond, OH groups, =C–H and C=O bond. Powder XRD studies indicated the formation of pure wurtzite hexagonal structure with particle sizes of 32 and 45 nm. UV-visible spectrophotometer showed absorbance peak in range of 375–378 nm. The antibacterial activity of the ZnO nanoparticles showed antibacterial activities against both Gram-positive (*Staphylococcus aureus*) and Gram-negative (*Pseudomonas aeruginosa*) microorganisms by disc diffusion method and also determined that the cytotoxicity was assessed by hemolytic activity. Our results have revealed that zinc oxide nanoparticles could elicit hemolysis and severely impact the proliferation of lymphocytes at all investigated concentrations (25, 50, 75, 100 µg/mL).

Keywords Zinc oxide nanoparticles · Chemical route · Sesbania grandiflora · Green route · Antibacterial activity · Hemolytic activity

1 Introduction

ZnO is an n-type semiconductivity metal oxide nanomaterial because of its large bandgap (3.37 eV) at room temperature (300 K) and high exciton binding energy (~ 60 meV) [1]. ZnO is a versatile material because of its physico-chemical properties such as mechanical, electrical, optical, magnetic, catalytic, strong piezoelectric and pyroelectric properties [2]. It has been wide range of various applications such as electronic devices, food packaging, waste water treatment and biomedical

applications like drug delivery, anticancer, antibacterial and antidiabetic activities, etc. [3].

Also according to the US Food and Drug Administration, zinc oxide and other four zinc compounds have been recorded as generally recognized as safe (GRAS) material (FDA 2015) [4]. There are numerous methods (physical, chemical and biological) that have been developed to fabricate ZnO nanoparticles: chemical and physical methods such as sol–gel, sputtering, hydrothermal, solvothermal, co-precipitation, chemical reduction, thermal decomposition and physical vapor deposition techniques [5]. Nanoparticles also derived from plants and microorganisms using biosynthesis route. The main reaction occurring in the biosynthesis of nanoparticles is oxidation/reduction process utilizing microorganisms, enzymes, plants and plant extracts that have been recommended as possible ecofriendly alternative methods to chemical and physical methods [6, 7]. Biosynthesis is one of the standard

✉ Vijaya P.P
vijayaparthasarathy@buc.edu.in

¹ Department of Nanoscience and Technology, Bharathiar University, Coimbatore, India

synthesis methodology for plant extract and has more advantages over other techniques such as no additional chemicals required, easily available, simple, cost effective, environmentally friendly and reliable method [8].

Among the biological sources for biosynthesis of nanostructures, plants have significant importance of a large spectrum of phytochemicals such as antioxidant flavonoids, glycosides, vitamins, terpenoids and tannins that act as reducing agents [9]. As demonstrated by Mahanty et al., the usage of ecofriendly biosynthesized nanoparticles is an alternative to the chemically synthesized nanoparticles. It has been demonstrated that plant extracts, which are known to shield a wide variety of biomolecules, may act as both reducing and stabilizing agent in the synthesis of nanoparticles [10].

Agathi or *Sesbania grandiflora* L. (Agast) is an outstanding little, freely spreading, legume plant of the Tropical Asia including India, Indonesia, Malaysia, Myanmar and Philippines [11]. It belongs to the family Leguminosae and its regular names are Agati or Sevvagatti. The plant contains rich in tanins, flavonoides, coumarins, steroids and triterpenes [12]. All parts of *Sesbania grandiflora* have been utilized experimentally as a conventional remedy in folk medicine to regard different diseases, for example, catarrh, diarrhea, fever, migraine, smallpox, sore throat and stomatitis [13] (Table 1).

The dried leaves are regularly used to make tea and are considered as great antibacterial, antihelminthic, antitumor and preventative properties [14]. The active ingredients of different parts of *Sesbania grandiflora* are olenolic acid and its methyl ester and Kaempferol-3-rutinoside present in flower. Saponin, sesbanimide, leucocyanidin and cyanidin are present in seeds. The bark contains tannins and gum [15]. According to the USDA supplement database, 100 g of *Sesbania grandiflora* leaves contains protein, carbohydrates, calcium, magnesium, potassium, sodium, selenium, vitamin C and iron [16] (Fig. 1).

The present study was carried out with the main objective to synthesize ZnO nanoparticles with enhanced antibacterial and hemolytic activity through chemical and green synthesis method using aqueous extracts of *Sesbania grandiflora*. The antibacterial activity of zinc oxide nanoparticles was investigated on both Gram-positive (*Staphylococcus aureus*) and

Gram-negative (*Pseudomonas aeruginosa*) common pathogenic bacteria. The hemolytic properties of zinc oxide nanoparticles on human RBCs are also investigated.

2 Materials and Methods

2.1 Materials

Zinc acetate ($\text{Zn}(\text{O}_2\text{CCH}_3)_2$), sodium carbonate (Na_2CO_3), sodium hydroxide (NaOH), nutrient agar, Luria-Bertani agar, phosphate-buffered saline, Triton X-100 and ethanol were purchased from Himedia Laboratories Private Limited, Mumbai, India. All glasswares were cleaned thoroughly with tap water followed by double distilled water and dried in hot air oven at 110–120 °C for 2–3 h prior to each experiment.

2.2 Plant Collection

Fresh leaves of *Sesbania grandiflora* leaves were collected from local market, Coimbatore. The collected plants were identified and authenticated (Reference No: BSI/SRC/5/23/2018/Tech/155) from Botanical Survey of India, Southern Regional centre, TamilNadu Agricultural University, Coimbatore.

2.3 Preparation of *Sesbania grandiflora* Leaf Extract

About 20 g of fresh and healthy leaves of *Sesbania grandiflora* (commonly called as Agathi) leaves was collected, washed thoroughly with running tap water to remove debris and other contaminated organic contents, followed by double distilled water and air-dried at room temperature. Finely cut into fine pieces and boiled with 200 mL double distilled water in a beaker at 80 °C for 30 min until the color of the water was turned to green color. The extract was cooled at room temperature and filtered using Whatman filter paper no.1 and extract was stored at 4 °C for further experiments. The extract used for the reduction of zinc ions (Zn^{2+}) to zinc nanoparticles (ZnO).

Table 1 Pharmacological activity of various parts of *Sesbania grandiflora* (Linn.)

Scientific name	Common name	Family	Parts used	Pharmacological activity
<i>Sesbania grandiflora</i>	Agati (Tamil)	Leguminosae	Bark	Anticonvulsant, antiulcerogenic activity
	Vegetable hummingbird (English)		Leaf	Anxiolytic, hepatoprotective, anticancer, antioxidant and antirolithiatic activity
	Hatga (Hindi, Marathi)		Flower	Anticancer, antimicrobial analgesic and anti-pyretic activity. used for anemia, fever and bronchitis
	Turi and geti (Malay)		Fruit	Anti-inflammatory and anti-pyretic
			Root	Anticonvulsant, antiulcerogenic activity

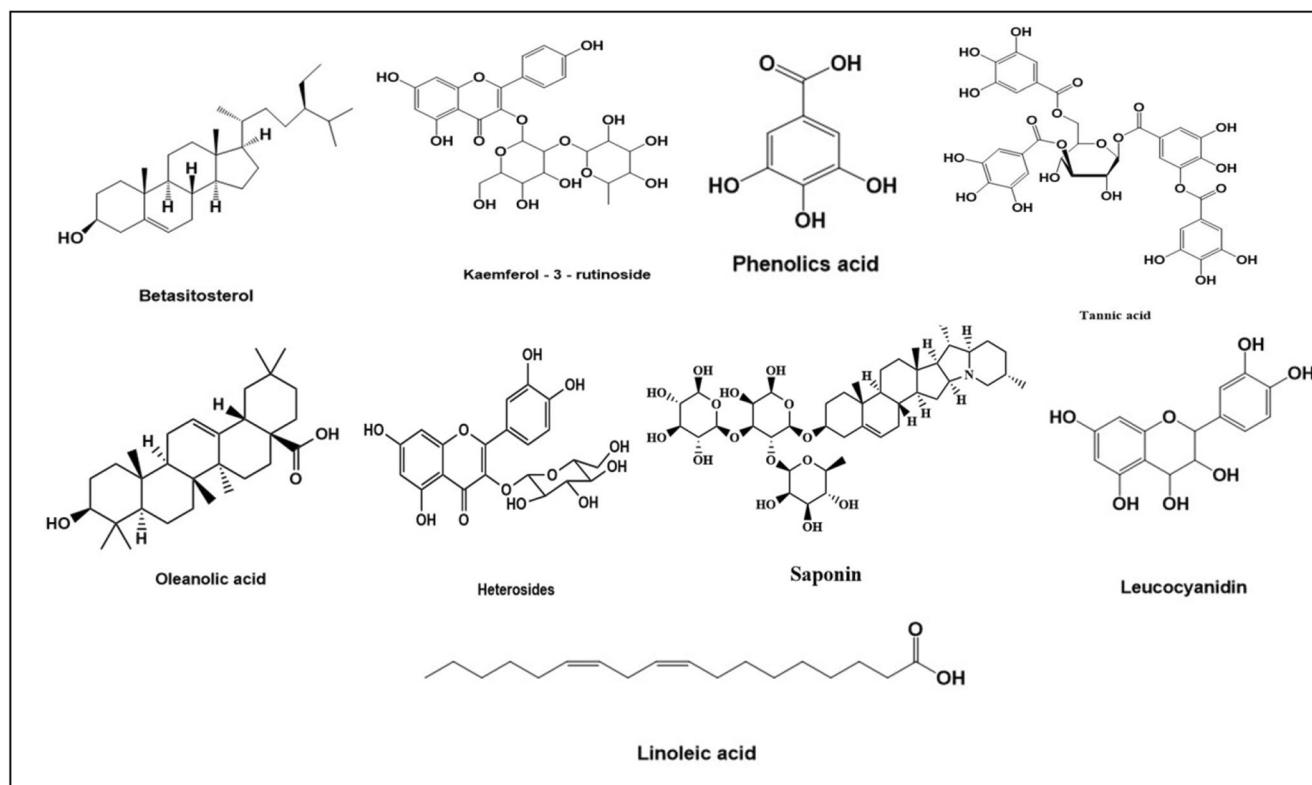
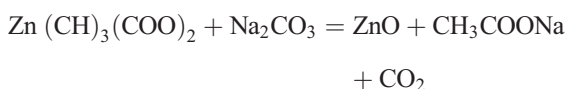


Fig. 1 Chemical structures of isolated constituents from *Sesbania grandiflora*

2.4 Synthesis of Zinc Oxide Nanoparticles by Co-precipitation Method

Zinc acetate is the chemical compound with the molecular formula $Zn(CH_3COO)_2$; it is used as a precursor in preparing semiconducting zinc oxide nanoparticles in chemical co-precipitation method. In a typical synthesis, 0.01 M aqueous solution of zinc acetate was dissolved in 50 mL of distilled water and added 0.02 M of sodium carbonate (Na_2CO_3) was also prepared in 50 mL of distilled water under magnetic stirring for 2 h, which resulted in the formation of a white suspension. The pH of the solution was adjusted to 5.5. After the reaction, the suspension was filtered washed with double distilled water and absolute ethanol several times, dried at 60 °C for 2 h and calcinated at 350 °C for 3 h to obtain the final product (i.e., ZnO nanoparticles).

The overall reaction mechanism of zinc oxide nanoparticles,



2.5 Green Synthesis of Zinc Oxide Nanoparticles

A total of 0.01 M solution of zinc acetate was dissolved in 50 mL of distilled water and kept in stirrer for 1 h, respectively. Then, 2 mL of leaf extract was added and heated to 80 °C with vigorous stirring for 30 min. The pH of the mixture was maintained at 8

and the solution was stirred continuously for 3 h. This mixture was heated until it reduced to a pale yellow color paste. This paste was then collected in a crucible and heated in a muffle furnace at 350 °C for 3 h to obtain the final product (i.e. ZnO nanoparticles).

2.6 Characterization of Zinc Oxide Nanoparticles

The crystalline structure of the nanoparticles was studied by an X-ray diffractometer (XRD; Rigaku Ultima IV) with $CuK\beta$ radiation at 25 °C and the structural assignments were made with reference to the JCPDS powder diffraction files. The intensity data was collected over a 2θ range of 20–80°. Functional group of the compound was examined by using Fourier transform infrared spectroscopy (SHIMADZU, INDIA). Morphology, topography and size of the sample were characterized by using field emission scanning electron microscope (FE-SEM FEI Quanta 250) and high-resolution transmission electron microscope (JEOL JEM 2100). Chemical composition of the sample was analyzed using energy dispersive spectrum (BRUKER INDIA). UV measurements were conducted using a Hitachi-U-2001 spectrometer.

2.7 Study of Antibacterial Activities of ZnO Nanoparticles

The antimicrobial activity of ZnO nanoparticles was evaluated against standard and clinical strains of Gram-positive and

Gram-negative bacteria (*S. aureus*: ATCC 4163 and *P. aeruginosa*: ATCC 6749) by the agar well diffusion method. The wells of 4 mm diameter were punched into the Luria-Bertani (LB) agar having the test microorganisms at concentrations of zinc oxide nanoparticles. The wells were filled with 100 μL of ZnO at the three different concentrations of 5 mg/mL, 10 mg/mL and 15 mg/mL. The plates were incubated for overnight at 37 $^{\circ}\text{C}$. Antimicrobial activity was evaluated by measuring the inhibition zone against the test microorganisms.

2.8 In Vitro Hemolysis Assay of the Nanoparticles

2.8.1 Isolation of Erythrocytes from Human Blood

Heparinized fresh human blood was taken from young, healthy, non-smoking individual (self-donor) volunteers. The hemolysis activity test was performed against both chemically and green synthesized zinc oxide nanoparticles. Two milliliters of blood was mixed with 0.2 M phosphate-buffered saline (PBS) (pH 7.0) and centrifuged at 2000 rpm for 15 min at 4 $^{\circ}\text{C}$ in a clinical centrifuge and the plasma and buffy coat were removed by aspiration. The erythrocyte pellet was washed thrice with PBS and containing red blood cells is further washed three times with PBS buffer and diluted with PBS at 1:4 ratio.

2.8.2 Treatment of Erythrocytes with ZnO NPs

In experiment, zinc oxide nanoparticles were dispersed in PBS buffer with different concentrations (25, 50, 75, and 100 $\mu\text{g}/\text{mL}$); then, 200 μL of RBC is added in all tubes (0.1% Triton X 100 and PBS buffer acts as a positive and negative control). The suspension is incubated at room temperature (37 $^{\circ}\text{C}$) on a platform shaker for 3 h. After that, the suspension is centrifuged at 6000 rpm for 15 min and absorbance is recorded at 540 nm (Fig. 2, 8).

The % hemolysis was calculated as

Hemolysis (%)

$$= \frac{\text{OD test sample} - \text{OD negative control}}{\text{OD Positive control} - \text{OD negative control}} \times 100$$

3 Results and Discussion

3.1 X-ray Diffraction Analysis

Figure 2, 3 shows the XRD pattern of ZnO (chemically and green) nanoparticles. All the diffraction peaks at angles (2θ) of 31.2 $^{\circ}$, 34.46 $^{\circ}$, 36.46 $^{\circ}$, 47.57 $^{\circ}$, 56.64 $^{\circ}$, 63 $^{\circ}$, 67.91 $^{\circ}$ correspond to the reflection from (100), (002), (101), (102), (110), (103), (112) crystal planes of the hexagonal wurtzite structure of

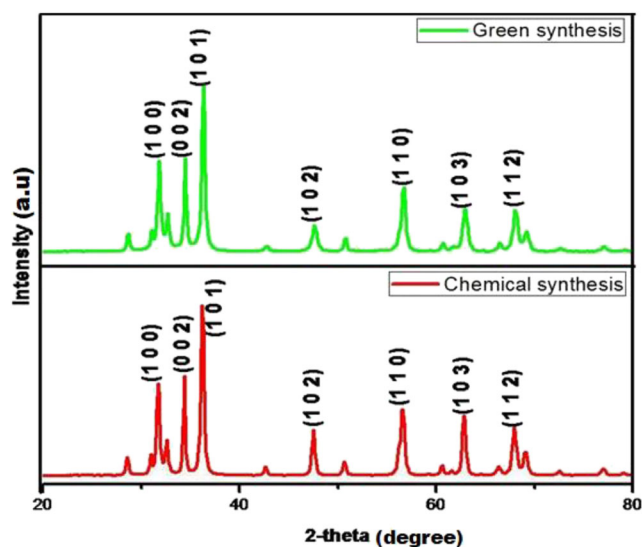


Fig. 2 The XRD pattern of ZnO nanoparticle synthesized from chemical and green synthesis method

ZnO nanoparticles (JCPDS No: 36-1451). The sharp and intense peaks are indicating that the ZnO nanoparticles were highly crystalline in nature. The diffraction peaks corresponding to the impurity were not found in the XRD patterns, confirming the high purity of the synthesized products.

The average crystalline size calculated using Debye-Scherrer formula,

$$D = \frac{K\lambda}{\beta \cos\theta}$$

where D is the average particle size, λ is the wavelength of X-ray used, K is the shape factor, β is the full line width at the half-maximum elevation of the main intensity peak, and θ is the Bragg angle. The size of the particles was calculated using

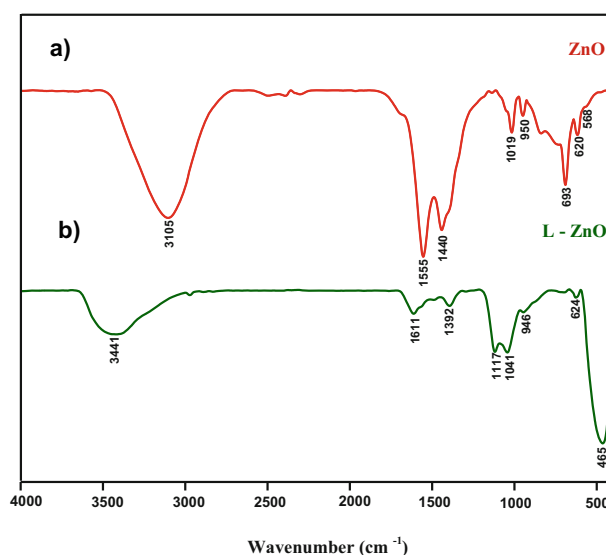


Fig. 3 a, b The FTIR spectrum of zinc oxide nanoparticles a chemical method and b green method

this equation found to be 32 nm and 45 nm for ZnO nanoparticles synthesized from chemically and green synthesis, respectively.

3.2 Fourier Transform Infrared Spectroscopy

Figure 3, 4 a and b show the FTIR spectra of both synthesized (chemical and green) zinc oxide nanoparticles, which were acquired in the range of 4000 to 450 cm^{-1} using the KBr method. The spectrum of zinc oxide nanoparticles showed the bands for the functional groups located at 3105, 3441, 1611, 1555, 1392, 1440, 1019, 1041, 1117, 950, 946, 693, 624, 620, 465, 568 cm^{-1} . The strong broad peaks in higher region at 3441 and 3105 cm^{-1} are due to the stretching vibration of hydroxyl (OH) groups. The peaks around 1611 and 1555 cm^{-1} are due to the C=O amide I and amide II group. The -C-H bending vibration band arises at 1440 and 1392 cm^{-1} . The C-O stretching vibration band arises at 1117, 1041 and 1019 cm^{-1} . The =C-H bending vibration band arises at 950, 946 and 693 cm^{-1} . The O-H bending vibration band arises at 624 and 620 cm^{-1} . The 568 and 465 cm^{-1} is attributed to the stretching vibration of Zn-O bonds and confirms the formation of product. FTIR analysis was done to identify the possible biomolecules responsible for the bio reduction of zinc oxide nanoparticles.

3.3 UV-Visible Spectrophotometer Analysis

The optical properties of zinc oxide nanoparticles were characterized using UV-visible spectrophotometer. Conducting electrons start oscillating at a certain wavelength range due to surface plasmon resonance (SPR) effect.

Figure 4 represents the UV-visible spectra of freshly prepared ZnO NPs and peak obtained at 375 nm clearly demonstrates the presence of ZnO NPs in the reaction mixture. Green synthesized zinc oxide formation was confirmed as the absorption peak (λ_{max}) was found near 378 nm. This

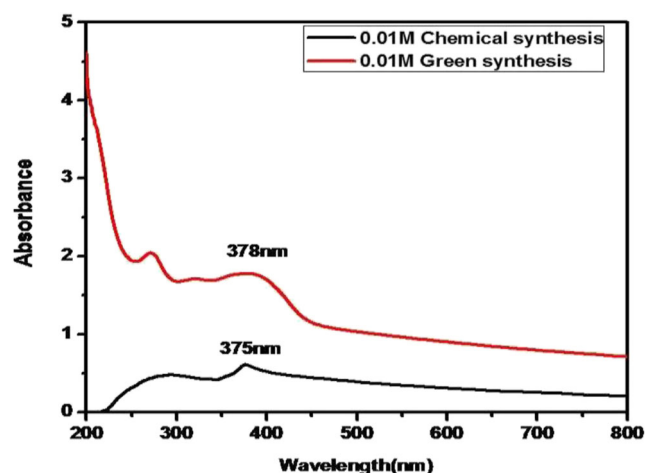


Fig. 4 The UV-visible spectra of chemically and green synthesized zinc oxide nanoparticles

could be due to the excitation of nanoparticles from ground state to excited state. From the UV-visible spectrometer analysis, it was concluded that zinc oxide nanoparticles had an intense absorbance at ~ 375 nm which indicates that the synthesized particles were photosensitive in UV region.

3.4 Field Emission Scanning Electron Microscopic Studies

The surface morphology analysis of synthesized zinc oxide nanoparticles was recorded through the field emission scanning electron microscopy (FESEM). Generally, the synthesized ZnO NPs were reported as homogeneous, agglomerated and without the presence of other dominating phases.

Figure 5 a–d show the as-prepared ZnO nanoparticles prepared by co-precipitation method at the pH range 8; a flakes-like structure was obtained. Figure 5 e–h show that the ZnO nanoparticles synthesized by the plant extract of *Sesbania grandiflora* is obtained from the proposed bio reduction method at the pH range 12; flower-like structure was obtained, and Fig. 5 i–l show the bio reduction method at the pH range 10; spherical-like structure was observed. From the images, we clearly identify that the pH plays the important role in morphology of the nanostructures.

3.5 Energy Dispersive Analysis of X-rays

The energy dispersive analysis of X-rays (EDAX) was carried out to determine the elemental composition and stereochemistry of the synthesized zinc oxide (chemically and biologically) nanoparticles. The energy dispersive spectra of the samples obtained from the FESEM–EDAX analysis shows that the sample prepared by above route has pure ZnO phases. Figure 6 a and b show that the quantitative and qualitative analysis of elements may be concerned in the formation of zinc nanoparticles. The elemental constitution of ZnO nanoparticles with two major peaks was found to have a weight percentage of zinc 79.29% and O 20.17% for chemical synthesis and zinc 77.80% and O is 22.2% for biosynthesis method.

The EDAX studies of Fig. 6a and b present three peaks between 1 Kv and 10 kV. The EDAX analysis confirmed the presence of the zinc and oxygen. The results indicated that the reaction product was composed of high purity zinc oxide nanoparticles.

3.6 HR-TEM Analysis of Zinc Oxide Nanoparticles

The morphology and size of prepared nanoparticles were analyzed by using HR-TEM. The fine powder of ZnO nanoparticles was dispersed in methanol on a carbon-coated copper grid, and the high-resolution transmission electron microscopy (HR-TEM) images were obtained with ultra high resolution at an accelerating voltage of 200 kV.

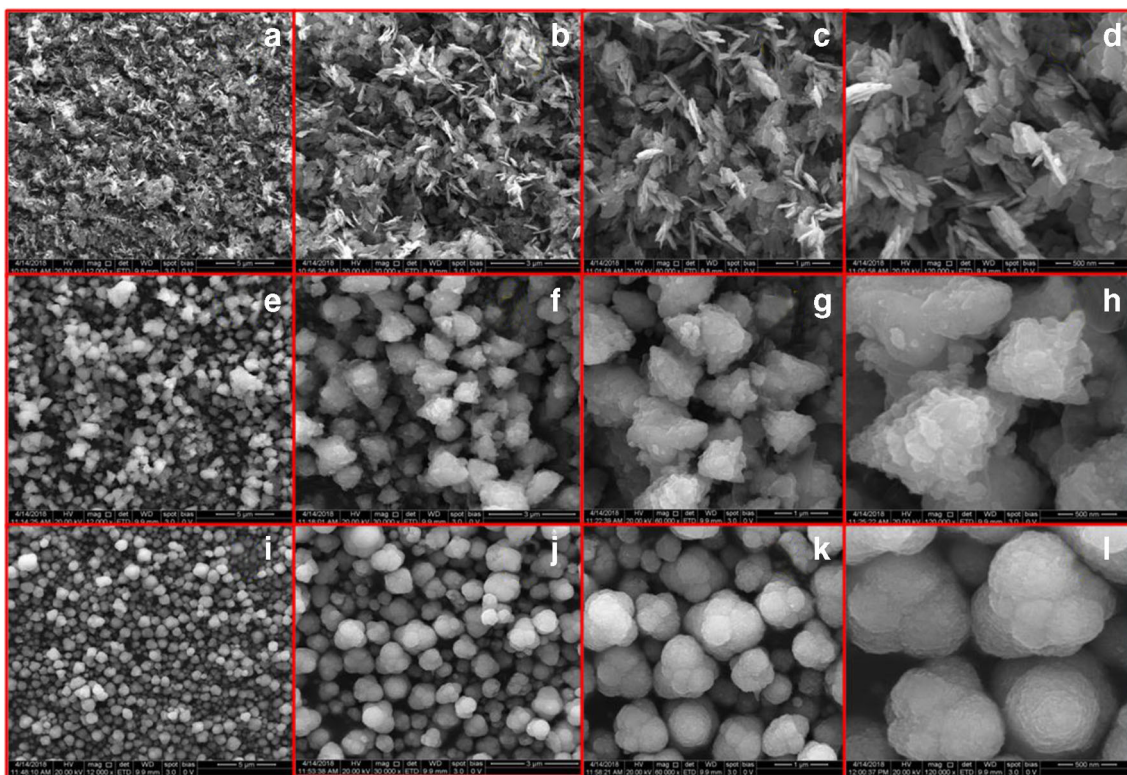


Fig. 5 The FESEM images (different magnifications) of ZnO nanoparticles

Figure 7a and b show the (HR-TEM) analysis of zinc oxide nanoparticles with different magnifications consisting of spherical in shape and it is well distributed without any aggregation. The size range of the particles is 45 nm. The crystallinity of the synthesized nanoparticles was also supported by the observed lattice fringes of 5 nm in HR-TEM images

shown in Fig. 7c. The selected area electron diffraction (SAED) pattern (Fig. 7d) shows the sharp spots indicative of polycrystalline nature with symmetrical orientation of ZnO nanoparticles in the sample.

The SAED pattern revealed that the diffraction rings of the synthesized ZnO exhibited Debye–Scherrer rings assigned

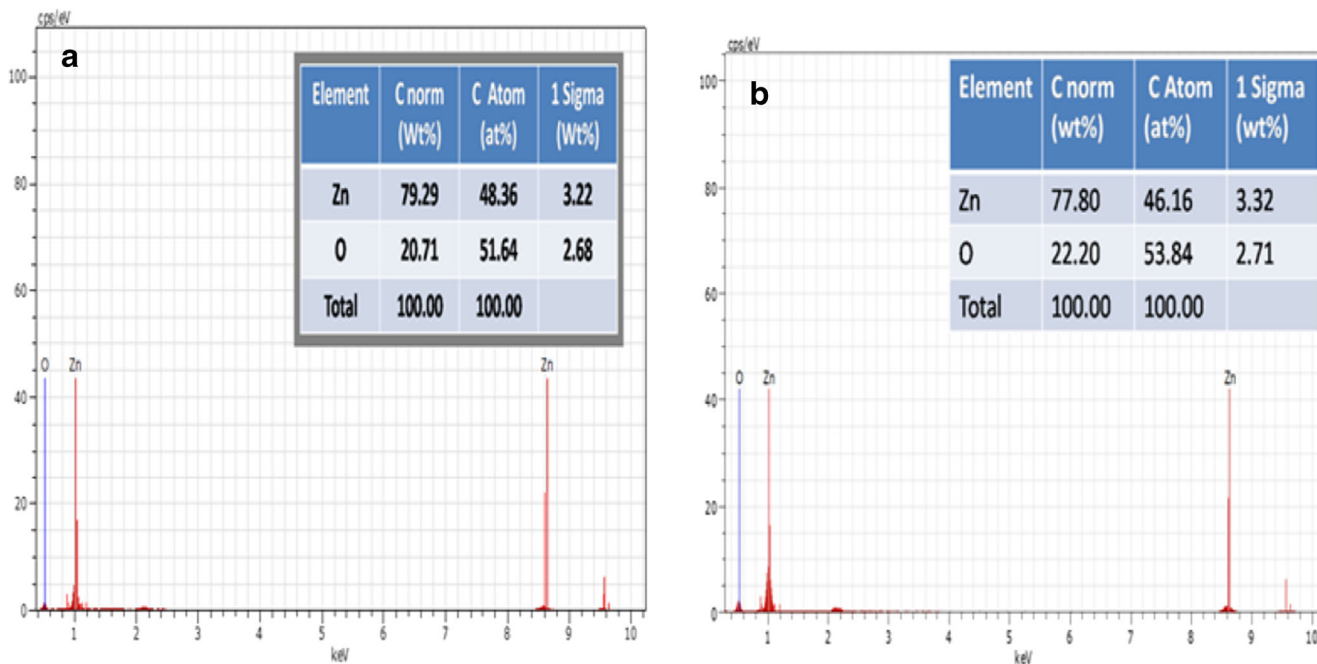
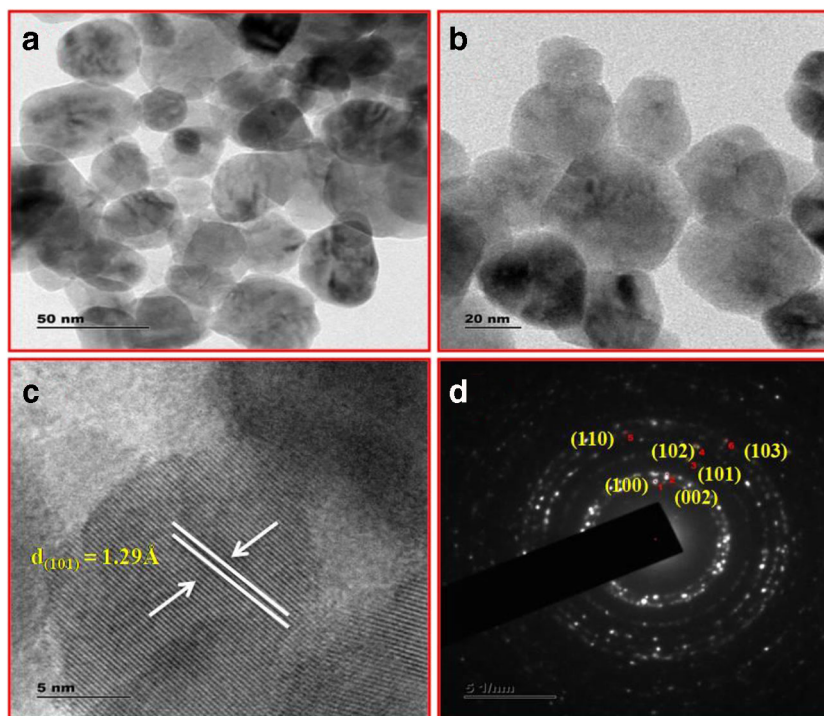


Fig. 6 a EDAX spectrum of chemically synthesized ZnO NPS. b EDAX spectrum of green synthesized ZnO NPs

Fig. 7 **a, b** The HR-TEM image of ZnO nanoparticles. **c** The individual particles (lattice image). **d** The selected area electron diffraction (SAED) pattern



(100), (002), (101), (102), (110), (103), respectively. The bigger particle is oriented in the (101) direction, and the attached neighboring particle on the left of this particle is oriented in the (002) direction. The measured distance from the HR-TEM image between the lattice planes is 1.29 Å in the (101) direction and 1.36 Å in the (002) direction, which is in very good agreement with that of the XRD pattern which also proves the hexagonal wurtzite structure of ZnO nanoparticles.

3.7 Hemolytic Activities of Zinc Oxide Nanoparticles

In Vitro Erythrocyte (RBC) Cells Induced hemolysis is considered to be a simple and reliable method for evaluating biocompatibility of nanomaterials. Nevertheless, a rare study has been conducted in this area that can provide a clear understanding of the toxic effect and mechanism of zinc oxide nanoparticle exposure to RBCs. All materials that enter into the blood get in contact with red blood cells (RBCs). To assess the impact of zinc oxide nanoparticles on erythrocyte, hemolysis test was performed by spectrophotometric measurement of hemoglobin release after exposure to various concentrations of zinc oxide nanoparticles.

Figure 8 shows the in vitro biocompatibility of the as-prepared zinc oxide (both chemically and green synthesized) nanoparticles. This result stated that ZnO NPs with different concentrations of 25, 50, 75 and 100 µg/mL showed lower hemolytic activity compared with positive control. The performance of hemolysis assay was tested by the negative control phosphate-buffered saline (PBS) and negative control Triton X-100. The interaction of ZnO nanopowders with

RBC revealed a hemolysis percentage of greater than 20 (chemical method) and 10 (green method) at a concentration of 100 µg/mL of ZnO nanopowders.

The observed hemolysis properties of these synthesized nanoparticles could be essentially attributed to their size, surface chemistry and physiochemical properties. Hemolysis process involves the denaturation of cells through the physiochemical interaction between nanoparticles and the cell surface. The mechanism of the hemolytic activity of the NPs depends on the increasing permeability to complete lysis of the cell. The cell lysis caused free radical formation and cell death and resulted in harmless RBC (erythrocyte) cell count. The detailed investigation of interaction between zinc oxide nanoparticles (size, dose) and RBC should be studied in in vitro and in vivo before their therapeutic usage. Therefore, within the limitation of this study,

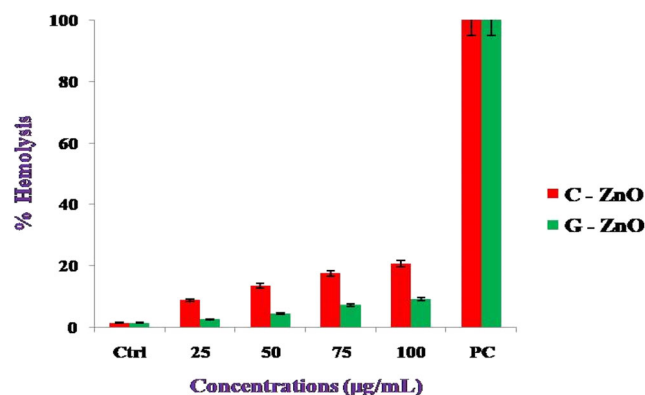
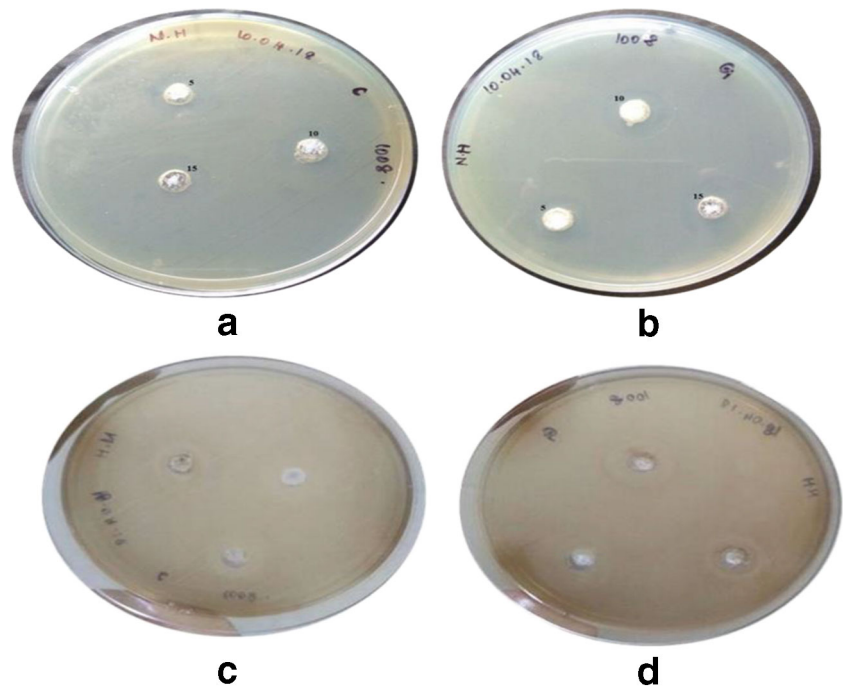


Fig. 8 The hemolytic activity of chemically and green synthesized ZnO nanoparticles

Fig. 9 **a, b** The antibacterial activity of ZnO nanoparticles against *S. aureus* and **c, d** the antibacterial activity of ZnO nanoparticles against *P. aeruginosa*



it can be concluded that the concentration of zinc oxide nanoparticles employed in the present antibacterial and anticancer activities is biocompatible.

3.8 Antibacterial Activity

Figure 9 shows that the antibacterial activity of ZnO (chemical and green) nanoparticles was evaluated by the agar well diffusion method against a Gram-positive (*Staphylococcus aureus*) and a Gram-negative (*Pseudomonas aeruginosa*) bacteria pathogens. The results of the inhibition zone were measured in millimeter (mm) range.

The presence of inhibition zone clearly indicates that the mechanism of the activities of ZnO nanoparticles, which involves disruption of the membrane with high rate of multiplication of surface reactive oxygen species and ultimately, goes to the death of pathogens. The zinc oxide nanoparticles show that significant growth inhibition in a size-dependent manner

under normal ambient lighting conditions. According to the Table 2 that shows the maximum zone of inhibition (ZOI) values, *P. aeruginosa* was more resistant to ZnO NPs than *S. aureus*. This resistance of *P. aeruginosa* compared to *S. aureus* (chemically and green synthesized NPs) might be due to the presence of cytochrome oxidase in *P. aeruginosa*.

The detailed possible mechanism of the bioactivity of ZnO is “based on the abrasive surface texture of ZnO NPs binding with bacterial surface is due to the electrostatic forces that directly kill bacteria”. Smaller particle size provides relatively larger surface area and higher amount of Zn atoms that trigger toxicity effect of ZnO towards the bacteria. The results for the green synthesized ZnO nanoparticles were comparable to the results obtained for chemically synthesized ZnO nanoparticles. ZnO nanoparticles synthesized using *Sesbania grandiflora* leaf extract were shown better result against *P. aeruginosa* and *S. aureus* than chemically synthesized ZnO nanoparticles.

Table 2 Zone formation shows the antibacterial activity against *Staphylococcus aureus*

Microorganisms	Concentrations (mg/mL)	Chemically synthesized ZnO nanoparticle (zone of inhibition) (mm)	Green synthesized ZnO nanoparticle (zone of inhibition) (mm)
<i>Staphylococcus aureus</i>	5	1.5	1.6
	10	1.6	1.8
	15	1.8	2.1
<i>Pseudomonas aeruginosa</i>	5	1.5	1.8
	10	1.8	2.0
	15	1.9	2.3

4 Conclusion

ZnO nanoparticles are successfully synthesized via two methods (chemical and green). Green synthesis of zinc oxide nanoparticles using *Sesbania grandiflora* leaves extract as a reducing and capping agent. It provides environmental friendly, simple and efficient route for synthesis of benign nanoparticles. The structure, morphology, chemical composition, functional groups and size of the prepared ZnO nanoparticles were characterized by XRD, HR-TEM, FTIR, UV-visible spectroscopy and FESEM and EDAX analysis. XRD results confirm that the average crystalline size observed from the intense planes was measured as 32 nm for chemical synthesis and 45 nm for green synthesis. The synthesized ZnO nanoparticles were of flower and flakes shaped and the estimated sizes were 70–150 nm. The green synthesis of ZnO nanoparticles was highly resistant compared to chemical synthesis in the antibacterial activity by using two test organisms *Staphylococcus aureus* and *Pseudomonas aeruginosa*. Although the antibacterial mechanism of ZnO nanoparticles is still unknown, the possibilities of membrane damage caused by direct or electrostatic interaction between ZnO and cell surfaces, cellular internalization of ZnO nanoparticles and the production of active oxygen species such as H_2O_2 in cells due to ZnO NPs. The hemolysis activity of the materials is found to be higher for chemical synthesized zinc oxide nanoparticles, while it is relatively lower for green-synthesized zinc oxide nanoparticles. Hence, it is concluded that interaction of ZnO NPs with lymphocytes stimulates excess ROS generation, induction of oxidative stress and genotoxicity in the cells. The results indicated that the effect of NPs on the cell toxicity and the oxidative mechanisms are both concentration- and shape-dependent, whereas the effects of NPs on human blood. Finally, the present study is so helpful and useful to the scientific community for using the ZnO NPs as the potent applications to the effective antimicrobial and anticancer agents for commercial biomedical applications

Acknowledgements The authors are grateful to DST-FIST and UGC SAP, New Delhi, India for the instrumentation facilities.

Funding statement Funding was provided by the Department of Science and Technology (DST) PURSE-Phase-II.

Compliance with ethical standards

Conflict of Interest The authors declare that they have no conflicts of interest.

Research Involving Human Blood Sample Healthy volunteer blood samples were collected into vials with heparin for anticoagulation according to Institutional Ethical committee clearance certificate at Bharathiar University, Coimbatore. All procedures performed in studies involving blood specimens were in accordance with the ethical standards of the institution or practice at which the studies were conducted.

Informed Consent Informed consent for donating blood samples from students for Research purpose.

References

1. Geetha, M. S., Nagabhushana, H., & Shivananjaiah, H. N. (2016). Green mediated synthesis and characterization of ZnO nanoparticles using *Euphorbia Jatropa latex* as reducing agent. *Journal of Science: Advanced Materials and Devices, 1*, 301–310.
2. Shekhawat, M. S. (2016). Biosynthesis of Zinc oxide nanoparticles using aqueous extracts of *Adhatoda vasica* Nees. *International Journal of biological papers, 1*, 9–15.
3. Jamdagni, P., Khatri, P., & Rana, J. S. (2018). Green synthesis of zinc oxide nanoparticles using flower extract of *Nyctanthes arbor-tristis* and their antifungal activity. *Journal of King Saud University – Science, 30*, 168–175.
4. Santhoskumar, J., Venkat Kumar, S., & Rajeshkumar, S. (2017). Synthesis of Zinc oxide nanoparticles plant leaf extract against urinary tract infection pathogen. *Resource-Efficient Technologies, 3*, 459–465.
5. Joel, C., & Badhusha, M. S. M. (2016). Green synthesis of ZnO Nanoparticles using *Phyllanthus embilica* Stem extract and their Antibacterial activity. *Der Pharmacia Lettre, Scholars Research Library, 8*(11), 218–223.
6. Dobrucka, R., & Dugazewska, J. (2016). Biosynthesis and antibacterial activity of ZnO nanoparticles using *Trifolium pratense* flower extract. *Saudi Journal of Biological Sciences, 23*, 517–523.
7. Matinise, N., Fuku, X. G., Kaviyarasu, K., Mayedwa, N., & Maaza, M. (2017). ZnO nanoparticles via *Moringa oleifera* green synthesis: Physical properties & mechanism of formation. *Applied Surface Science, 406*, 339–347.
8. Mohammadi, C., Mahmud, S. A., Abdulla, S. M., & Mirzaei, Y. (2017). Green synthesis of ZnO nanoparticles using the aqueous extract of *Euphorbia petiolata* and study of its stability and antibacterial properties. *Moroccan Journal of Chemistry, 5*(3), 476–484.
9. Enhanced antibacterial activity of zinc oxide nanoparticles synthesized using *Petroselinum crispum* extracts, Manuela Stan, Adriana Popa, Dana Toloman, Teofil-Danut Silipas, Dan Cristian Vodnar, and Gabriel Katona.
10. Sarvade, S. (2014). *Sesbania grandiflora* (L.) Poiret: A Potential Agroforestry Tree Species. *Popular Kheti, 2*(3).
11. Noviany, H., Hasnah, O., Suriyati, M., Keng, C. W., Khalijah, A., Anis, S., Mohd, Z. (2012). The Chemical Components of *Sesbania grandiflora* Root and Their Antituberculosis Activity. *Pharmaceuticals (Basel), 5*(8):882–889.
12. Bahera, M., Karki, R., & Shekar, C. (2012). Preliminary Phytochemical Analysis of Leaf and Bark methanolic extract of *Sesbania grandiflora*. *The Journal of Phytopharmacology (Pharmacognosy and Phytomedicine Research), 1*(2).
13. Hasan, N., Osman, H., Mohamad, S., Chong, W. K., Awang, K., & Zahariluddin, A. S. M. (2012). The Chemical Components of *Sesbania grandiflora* Root and Their Antituberculosis Activity. *Pharmaceuticals, 5*, 882–889.
14. Arfan, N. B., Julie, A. S., Mohiuddin, A. K., Khan, S. A., & Labu, Z. K. (2016). Medicinal Properties of the *Sesbania grandiflora* Leaves. *Journal of Biomedical Science, 8*(6), 271–277.
15. Wagh, V. D., Wagh, K. V., Tandale, Y. N., & Shubhangi, A. (2009). Salve Phytochemical, pharmacological and phytopharmaceutics aspects of *Sesbania grandiflora* (Hadga): A review. *Journal of Pharmacy Research, 2*(5), 889–892.

16. Karmakar, P., Singh, V., Yadava, R. B., Singh, B., Singh, R., & Kushwaha, M. (2016). Agathi [*Sesbania grandiflora* L. (Agast)]: Current Status of Production, Protection and Genetic Improvement. *National Symposium on Vegetable Legumes for Soil and Human Health*.

Publisher's Note Springer Nature remains neutral with regard to jurisdictional claims in published maps and institutional affiliations.